Article:
Ghanbarzadeh, A orcid.org/0000-0001-5058-4540, Piras, E, Wilson, MCT orcid.org/0000-0002-1058-2003 et al. (2 more authors) (2019) Numerical Study of the Effect of Tribofilm Kinetics and its Hardness on the Roughness Evolution of the Substrate in Boundary Lubrication Regime. Tribology Transactions, 62 (5). pp. 747-759. ISSN 1040-2004

https://doi.org/10.1080/10402004.2019.1615160

Numerical Study of the Effect of Tribofilm Kinetics and its Hardness on the Roughness Evolution of the Substrate in Boundary Lubrication Regime

Ali Ghanbarzadeh[1], Elio Piras[2], Mark C.T. Wilson[1], Ardian Morina[1], Anne Neville[1]

[1]Institute of Functional Surfaces, School of Mechanical Engineering, University of Leeds, Leeds, UK

[2]NYCO, 66 avenue des Champs-Elysées, Paris cedex 08 France

Abstract

A tribochemical modelling framework that considers the growth of tribofilm on the contacting surfaces has been used in this work. The model couples a fast contact mechanics model with the thermodynamics of interfaces and captures the growth of the tribofilm on the asperities. The model was shown to be able to capture the dynamics of a tribosystem and the evolution of surface topography. The model considers the effect of plastic deformation and wear in modifying the surface geometries. In a recent work of the authors, (Ghanbarzadeh et al. in Wear 2016) the same numerical model was validated against experiments of the Micropitting Rig (MPR) and the wear, topography and tribofilm thickness results were compared. In this work, while the validation of the model is presented, the effect of tribofilm kinetics and its hardness have been numerically studied to assess the evolution of surface roughness in a rolling sliding contact. Results suggest that the kinetics of the tribofilm growth significantly influences the roughness evolution with higher kinetics resulting in a rougher interface. Similarly the tribofilm hardness affect the roughness evolution and are more influential in the later stages of roughness evolution.

Key words: Surface Roughness, Boundary Lubrication, Tribochemistry, Wear, ZDDP

1 Introduction

Wear of materials is still a big problem in engineering systems where material loss occurs due to various mechano-chemical processes on the surfaces of contacting bodies. Wear has a significant impact on the reliability of machine components and is one of the most important factors in design. At the theoretical level, a recent review [1] highlighted the enormous complexity of even a very simple tribological process. Friction and wear are interlinked at all length scales and studying them requires an in-depth understanding of all the non-equilibrium processes occurring at the molecular level to determine what happens at the macroscopic level. Therefore it is a complex task to predict wear and friction at different scales. Numerous

attempts have resulted in various aspects of this problem being investigated and many system-dependent empirical and semi-empirical models have been developed [2, 3].

One important characteristic of a tribological system is the film thickness parameter known as the λ ratio which is a representation of the severity of the contact. Traditionally, λ ratio was used by designers of machine elements as a guide for selecting the right lubrication and material parameters [4, 5]. This is a fairly good design parameter for less severe contacts e.g. contact in ElastoHydrodynamic Lubrication (EHL) and Hydrodynamic Lubrication (HL). When the contact severity is greater, the lubricant film cannot sustain the load and the contact pressure will be mainly carried by the surface asperities. The concept of minimum film thickness will be invalid but λ ratio will still be a good representation of the severity of the contact. In the boundary and mixed lubrication regimes, prediction of the dynamics of surface topography evolution will result in a better estimation of the contact pressure and the contact conformity. Running-in is an important phenomenon in the wear and friction process as the majority of the surface modifications happen in this phase [6]. It has been shown that the running-in is a complex phenomenon where physical and chemical changes happen very quickly at the interface [7, 8].

A range of experimental work has investigated changes in surface roughness during running-in of tribological contacts. Karpinska [9] studied the evolution of surface roughness over time for both base oil and base oil with Zinc Dialkyldithiophosphate (ZDDP) antiwear additive. She also studied the wear of surfaces at different instants during running-in. It was suggested that a ZDDP tribofilm significantly affects the topographical changes of surfaces during running-in. From a design point of view, it is important to be able to predict the topography evolution of surfaces in order to be able to predict their performance under different lubricating conditions. Several previous works consider wear prediction using Finite Element Methods (FEM) [10-13], Boundary Element Method (BEM) [14-16] and combined methods [17, 18].

Due to complicated physical and chemical interactions in the boundary lubrication regime, it is a difficult task to predict surface roughness changes accurately while considering all the possible mechanisms such as tribofilm formation, its removal, material transformations, wear, friction, energy dissipation etc. A few recent works have considered the effect of protective surface lubricant films in the wear calculations [19-23] based on simplifications of tribofilm kinetics, mechanical properties and tribofilm friction. Since then models of the kinetics of tribochemical reactions [24-26] have been developed based on the hypothesis of shear-induced

tribochemical reactions. In an earlier work by the authors of this paper [22, 27], a tribochemical kinetic model was developed based on the thermodynamics of interfaces and a fitting parameter was introduced that was responsible for the effect of mechanical rubbing on induction of the tribochemical reactions. The model was an engineering approach to use the experimental macroscopic tribofilm growth data at the microscopic asperity-scale level and predict the dynamics of the tribosystem with respect to surface roughness and contact mechanics. Although it was semi-deterministic and dependent on experimental data, it was a good approach to couple tribochemistry and contact mechanics.

In another work [28], the effect of tribochemical protective antiwear films on the roughness evolution in the boundary lubrication regime was investigated. The surface topography evolution was reported to be due to three main components: plastic deformation, wear and tribofilm growth. The prediction results were validated against the experimental results of a micropitting rig. In the current work, while the validation of the model for one case against the experimental measurements is presented for reference, the previous model has been explored further to study the effect of the tribofilm kinetics and the tribofilm hardness in the prediction of roughness evolution of the surfaces. Experimental investigation of the effect of tribofilm kinetics and its mechanical properties is difficult as there is very limited control of these variables and they can usually be measured only post-experiments. Therefore, in this paper, the effect of these parameters is investigated numerically and only the experimental validation of topography evolution for one case is presented. The results of this paper will perhaps persuade designers to take kinetics of the anti-wear tribofilm as a design parameter and are illustrating a potential opportunity to steer future experiments. The summary of the model is presented in Section 2 followed by the system configuration, the experimental methodology and the experimental results in Section 3. Section 4 presents the validation of the model by means of one set of experiments and numerical results of the effect kinetics and hardness are reported in Section 5.

2 Summary of the model

The numerical model used here consists of the following three main components:

- An in-house contact mechanics solver with elastic-perfectly plastic model.
  A robust contact mechanics solver is necessary to calculate the contact pressure distribution and contact temperature.
- A semi-analytical time and space-dependent tribofilm growth model.

In order to study the effect of tribochemistry, the dynamics of the tribofilm growth at the interfaces should be captured.

- A modified Archard's wear model taking into account the local thickness of the tribofilm.

  The effect of the tribofilm dynamics in reducing wear is important. The chemical composition and hardness of the tribofilm evolve in time with pressure, temperature and rubbing time and this should be somehow captured in the model by only modifying the Archard's wear equation.

The components of the numerical model have been summarised in a flowchart as shown in Figure 1.

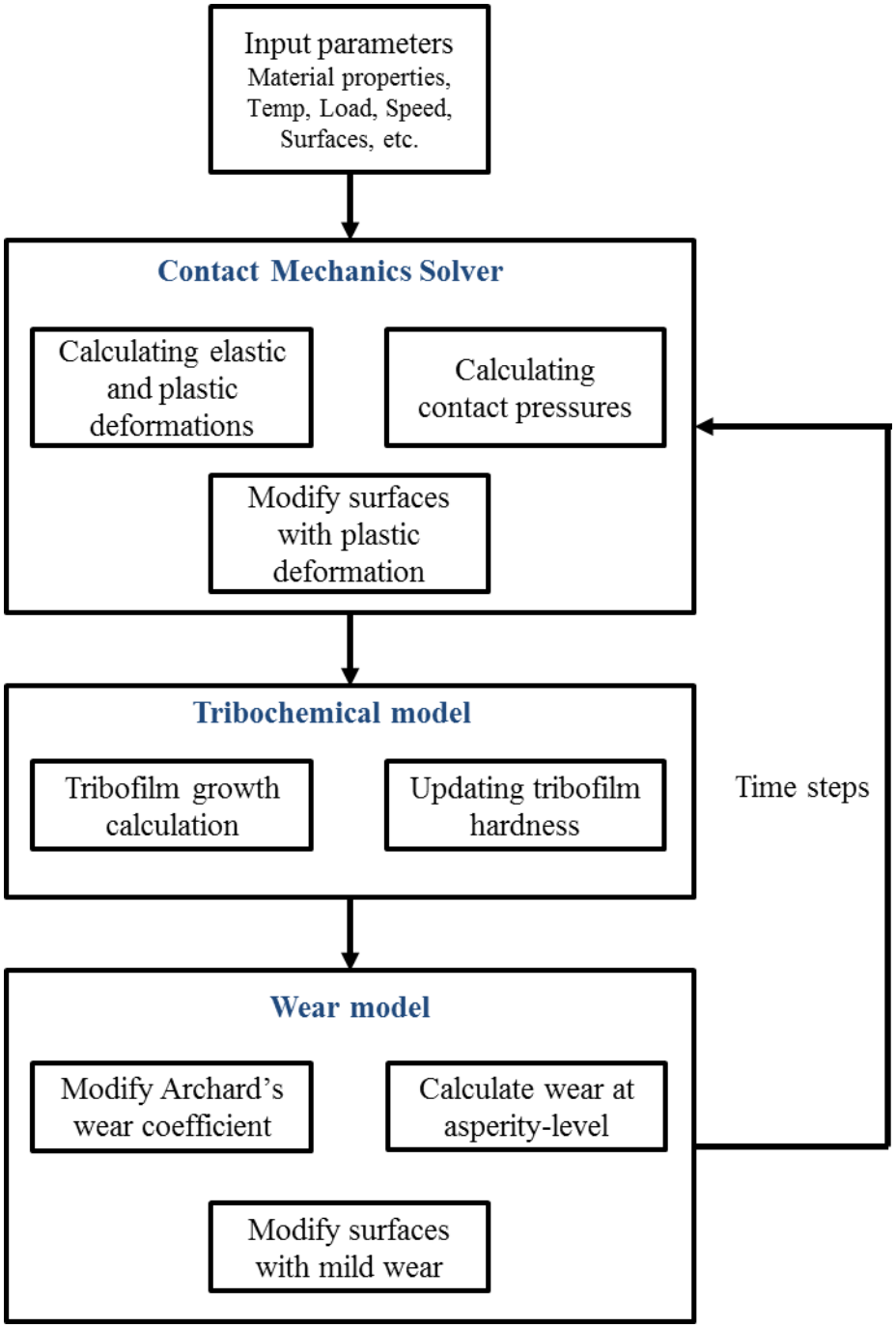

Figure 1 Flowchart of the numerical model

2.1 Contact mechanics solver

When the rough surfaces of two materials come into contact, individual asperities will sustain the load and the real area of contact will be significantly smaller than the nominal Hertzian contact area. Surfaces will be deformed with respect to the inhomogenous contact distribution. The composite deformation of the surfaces $u_e(x, y)$ due to the applied load of $p(x, y)$ can be calculated by the linear convolution according to Boussinesq-Cerruti theory:

$$u_e = K * p_d = \int_{-\infty}^{+\infty} \int_{-\infty}^{+\infty} K(x-\xi, y-\eta)\, p(\xi,\eta)\, d\xi\, d\eta \qquad (1)$$

in which x and y are two-dimensional coordinates, K is the convolution kernel and can be calculated from the half-space approximation as the following:

$$K(x-\xi, y-\eta) = \frac{1}{\pi E^*} \frac{1}{\sqrt{(x-\xi)^2 + (y-\eta)^2}} \qquad (2)$$

where E^* is the composite elastic modulus of both materials ($\frac{1}{E^*} = \frac{(1-\nu_1{}^2)}{E_1} + \frac{(1-\nu_2{}^2)}{E_2}$). Here, ν_1, ν_2, E_1 and E_2 are the Poisson's ratio and Elastic Modulus of material 1 and 2 respectively. For the contact of two rough surfaces, one can consider the composite roughness of the two contacting surfaces and a rigid plane to calculate the contacting points [29]. By movement of the rigid body in the normal direction, the interference (i) between the contacting surfaces can be obtained (see Figure 2). For the nodes experiencing contact, the elastic deformation must be equal to the body interference and the pressure is generated at the asperity. The summation of the pressures on the nodes must also be equal to the applied load. Therefore, the set of equations for the contact of rough surfaces is as follows:

$$u(x,y) = i(x,y) = Z(x,y) - D(x,y) \qquad \forall (x,y) \in A_e \qquad (3.1)$$

$$p(x,y) > 0 \qquad \forall (x,y) \in A_e \qquad (3.2)$$

$$W = \iint p(x,y)dxdy \qquad (3.3)$$

where i is the asperity interference, Z is the composite surface roughness height, D is the distance between reference plane and the rigid plane and W is the total applied load.

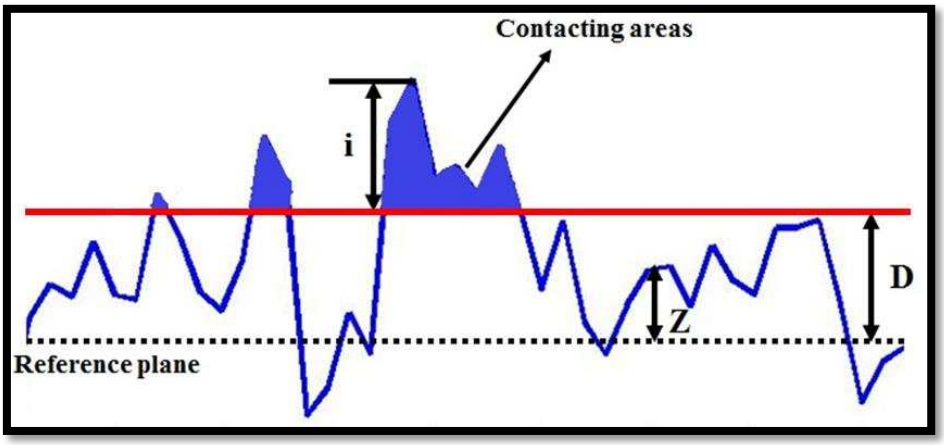

Figure 2 Schematic of the contact of rough surfaces

For the case of elastic-perfectly plastic contacts, there will be an additional criterion that limits the contact pressure to a maximum yield pressure (p_y) and Equation 3.2 will be converted to $0 < p(x, y) < p_y$. It is considered that the nodes which are experiencing pressures very close to p_y will not contribute to the elastic deformation calculation of the surface (Equation 1) and they are free to flow from the moment the pressure reaches the yield value. This is a simplification of the real system as the work-hardening is neglected and also sub-surface deformations are not considered. However, it is a fairly fast method to calculate the plastic deformation for rough surface contact mechanics. A simple heat transfer model was used in this work to calculate the flash temperatures on the contacting asperities via Blok's theory [30]. The model is based on quasi-steady-state models presented by Tian and Kennedy [31] which uses the following equation for the square shaped heat source:

$$T_{flash} = \frac{2qb}{K\sqrt{\pi(1.011 + pe)}} \qquad (4)$$

where b is the contact width, K is the thermal diffusivity ($K = \frac{k}{\rho C}$), Pe is the Peclet number ($Pe = \frac{bV}{K}$), q is the frictional heating ($q = \mu.P.V$) where μ, P and V are the coefficient of friction, contact pressure and sliding velocity respectively. The flash temperature calculated at the computational nodes will be then used to predict the tribofilm growth explained in the next section.

2.2 Tribofilm growth model

The tribofilm growth model was initially developed [22, 27] for antiwear additives and considered both formation and removal of the tribofilm. Due to the complex physics of the combined effect of formation and removal, the model used a fitting calibration approach to extract some parameters from the experiments. This approach limits the applicability of the model because it was only valid for a certain lubricant additive (ZDDP), however it was the first attempt to consider both formation and removal of such tribofilms at the asperity level. Computational nodes are in the range of micrometre (size of nodes are given later in Section 2.4) and the tribofilm can be formed on every computational node that is in contact. The film thickness (h) model is a function of time (t), temperature (T) and some other parameters that take into account the effect of mechanical rubbing (x_{tribo}), maximum tribofilm formation thickness (h_{max}) and tribofilm removal (C_3 and C_4). The growth model was formulated as the following:

$$h(t) = h_{max}\left(1 - e^{\left(-\frac{k_1 T}{h'}.x_{tribo}.t\right)}\right) - C_3(1 - e^{-C_4 t}) \qquad (5)$$

in which k_1 and h' are the Boltzmann and the Planck constants respectively. The term x_{tribo} was introduced by Bulgarevich et al. [32, 33], to account for the effect of mechanical rubbing on the initiation of tribochemical reactions. In principle, this term relates to the proportion of transition states in the tribochemical reaction that result from mechanical activation; in practice it is a fitting parameter to be calibrated via experiments providing in situ measurements of tribofilm thickness. A detailed discussion on the development of the growth model can be found in Refs [22, 27, 32-34]. This growth model was used on the asperity level and the inhomogenous time and space-resolved growth of the tribofilm was predicted. This was the first step to mechanistically implement tribochemistry into deterministic tribology models. In principle, the model of Equation 5 can be applied to any lubricant additives that are part of the tribochemical reactions. It should be noted that both formation and removal of the tribofilm are considered in this model. The model was initially developed for antiwear additives (ZDDP in particular) since their kinetics were studied more widely in the literature. It is important to highlight that x_{tribo} cannot be predicted in the current state of the model since it is related to the complicated physical and chemical properties of the interfaces. These properties of interfaces govern the kinetics of tribochemical reactions. One of such properties is the chemical nature of the lubricant additives. There is no means for accommodating chemical structure of the additives or their tribofilms and their interactions with substrates into the numerical model and further ab-initio studies of tribochemical reactions and multi-scale modelling approaches will add further insights into this. In the present form of the model, the term x_{tribo} cannot be directly correlated to the external force quantitatively and future single-asperity studies will be needed to study the effect of external force in more detail. In order to move forward and investigate the effect of tribofilm on wear of boundary lubricated contacts, different physical properties such as hardness of the film and its kinetics need to be studied numerically.

2.3 Modelling wear

It is important to differentiate the removal of the tribofilm that is obtained from the second part of Equation 5 and the wear of the substrate which is the wear of the material underneath the tribofilm. Hereafter, the term wear will refer to the mild wear of the substrate. Studies of ZDDP tribofilms on steel show that the tribofilm contains substrate atoms at a concentration that decreases towards the top of the tribofilm. Hence material from the substrate is consumed in forming (and maintaining) the tribofilm, and therefore if part of the tribofilm is removed due to the contact, this corresponds to an effective removal of material from the substrate. This principle is the basis of the mild wear model of Bosman et al. [35], who linked the rate of

substrate wear to the rate of tribofilm removal by considering the volumetric percentage of iron as a function of depth in the tribofilm, and the work of Akchurin et al. [23], who calculated the growth of the tribofilm deterministically using a linear wear model with respect to the tribofilm thickness that was validated against the experimental work of Ghanbarzadeh et al. [22].

Therefore, referring to the same tribochemical wear explained above, the link between the substrate wear and the tribofilm thickness takes a linear form in this paper. The details are explained elsewhere [22] but, in brief, the wear model is a modified version of Archard's wear equation in which the local wear coefficient is related to the local tribofilm thickness. The local wear depth of each point at the surface is given by:

$$\Delta h(x,y) = \frac{K(h)}{H}.P(x,y).\Delta t.v \qquad (6)$$

in which H, $K(h)$, P, v, and Δt are the material hardness, dimensionless Archard's wear coefficient, local contact pressure, sliding speed, and time step respectively. All the parameters in Equation (6) except $K(h)$ are calculated in the contact mechanics simulation. It is assumed that the coefficient of wear is at its maximum for steel-steel contact (i.e. when no tribofilm is present) and at its minimum when the tribofilm has its maximum thickness. Assuming, in addition, a linear variation with tribofilm thickness h, the coefficient of wear is given by:

$$K(h) = K_{steel} - (K_{steel} - K_{min}).\frac{h}{h_{max}} \qquad (7)$$

where $K(h)$ is the coefficient of wear for a substrate covered by a tribofilm with thickness h. K_{steel} and K_{min} are the coefficients of wear for steel and for the maximum ZDDP tribofilm thickness respectively, and h_{max} is the maximum tribofilm thickness. The values of K_{steel} and K_{min} are determined from calibration experiments as described in Refs [22, 28]. Wear measurements were conducted at different time periods of running the experiments and the initial wear rate was obtained and set as K_{steel} and the steady-state wear rate was set as K_{min} where a fully-formed tribofilm was separating the surfaces.

2.4 Numerical discretisation

In order to solve the set of Equations 1-3, the numerical domain should be discretised into rectangular elements of similar size in which the contact pressure can be assumed to be constant. In discretised form Equation 1 becomes:

$$u_{(i,j)} = K * p_d = \sum_{k=1}^{N}\sum_{l=1}^{N} K(i-k, j-l)\, p(k,l) \qquad i,j = 1,2,\dots,N \qquad (8)$$

where $p(k,l)$ is the constant pressure acting on the element centred at (k,l). Solving Equation 8 along with Equation 3 requires an iterative process to modify the contact pressures and finding the corresponding surface deformations. This can be solved using the matrix inversion process and requires $N^2 \times N^2$ operations. Using the DC-FFT algorithm widely reported in the literature [36-38] can reduce the computational demand dramatically. Equation 8 will be then converted to:

$$u_{(i,j)} = IFFT\left[\widetilde{K}_{i,j}.\tilde{p}_{i,j}\right] \qquad i,j = 1,2,\ldots,N \qquad (9)$$

where $\widetilde{K}_{i,j}$ and $\tilde{p}_{i,j}$ are the Fast Fourier Transforms of the influence coefficient and contact pressure matrices and are multiplied element-by-element. The FFT-based convolution is accompanied by periodicity errors that can be minimized by means of zero-padding contact pressure matrix (doubling the domain and putting zero pads in both x and y directions) and wrap-around [38]. It should be noted that dealing with 3-dimensional surfaces (i.e. topography varying in both x and y), both contact pressure and influence matrices should be expanded in both x and y directions. In order to increase the applicability and efficiency of the method, the number of nodes chosen for the numerical study should be a power of 2. The surfaces used in this study consist of 512×512 nodes of 0.25 μm size.

3 Experimental set up

In this work, experimental tribological tests were carried out using the MPR. The schematic representation of the MPR is shown in Figure 3. This is the same contact configuration as the one reported in Ref [28].

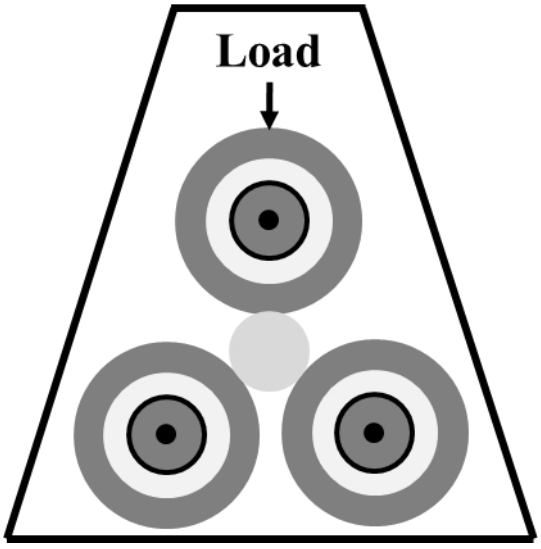

Figure 3 Schematics of the load unit of the Micropitting Rig (MPR)

Micropitting rig is comprised of a load unit that contains a roller of 12mm in diameter with the root mean square roughness (R_q) value of 50±10 nm and three larger cylindrical rings with R_q value of 600±50 nm. The material used for ring and the roller was Steel AISI 52100 that had elastic modulus of 210 GPa and Poisson's ratio of 0.27. As can be seen in Figure 3, due to the number of parts and size differences, the roller will experience more loading cycles than the individual rings (~13.5 times more). The experiments were conducted at a maximum contact pressure of 1.5 GPa. Since there are independent motors for rings and the rollers, the rig can simulate a sliding and rolling condition. The Slide-to-Roll Ratio (SRR) used in this study was 2% with the entrainment speed of 1m/s. The experimental parameters used in this study are reported in a table in Ref [28]. The lubricant used in this study was a poly-alpha-olefin, PAO as a base with viscosity of 9.84 cSt at 100ºC and 56.2 cSt at 40ºC. 1wt% (1.2% molar fraction) of primary zinc dialkyl dithiophosphate (ZDDP) was added to the base. The temperature of the oil bath was controlled at 90ºC.

In order to investigate the evolution of surface roughness, tests with different time durations were carried out and the surfaces were used for surface analysis. The Root Mean Square roughness of surfaces were then measured using White Light Interferometry (Wyko NT1100). After every test, samples were cleaned using ultrasonic bath for 5 minutes using Acetone as the solvent and ethylenediaminetetraacetic acid (EDTA) was used to remove any tribofilm from the surfaces. Zinc polyphosphates are known to have transparent properties therefore giving misleading results during light interferometry [39]. The roughness of roller and the rings were measured at 5 different positions in the wear track and the tests were repeated 3 times and an average value is reported here. Examples of such measurements are presented in Figure 4.

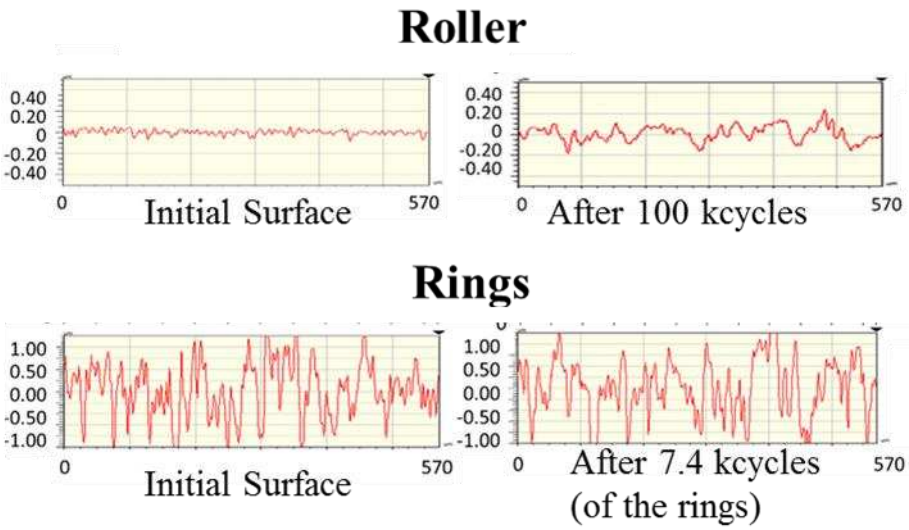

Figure 4. Example of Wyko roughness measurements (all values are in micro metre). Rolling/sliding direction is perpendicular to the plane

3.1 Experimental results

The roughness measurements of the rings and the rollers are presented in Figure 5. Experiments were conducted for different initial roughness values of the rings (rollers all have the same initial RMS) as reported in Ref [28]. For validation purposes, the roughest ring surface ($R_{q\,\mathrm{rings}}$=600 nm) was selected since it assures a contact in the boundary lubrication regime. It is interesting to see that the roughness of the rougher surface decreases rapidly in the initial stages of the contact and then increases gradually. On the other hand, the roughness of the roller increases gradually. This is a well-known observation that the roughness of two contacting surfaces tend to converge to similar values close to each other (surfaces conform to each other)[40] . It can be observed that due to the high value of roughness on the ring, the severity of the contact is high (boundary lubrication) and surfaces experience high plastic deformation at the start of rubbing. The plastic deformation dramatically changes the surface topography at the start of the rubbing. The tribofilm will form on the surfaces of both materials and this will delay the further smoothening of surfaces which will be followed by mild wear. Detailed chemical and physical analysis of the effect of the tribofilm on the roughness evolution of the surfaces are presented in the earlier work were SEM micrograph of the wear scar and chemical analysis confirm the morphology and chemistry of the tribofilm formed on the wear track [28].

4 Numerical validation

The configuration of roller and ring surfaces used in the contact mechanics simulation are shown in Figure 6. In order to simulate the rolling and sliding contacts, the surfaces of the ring and the roller should move relative to each other in the tangential direction. This is possible by shifting the matrices of surface asperity heights. Because of the high number of loading cycles it is not possible to simulate all the loading cycles, even with the smallest appropriate domain size. Selection of the size of the wear time-step is dependent on several parameters, the most important of which are the contact pressure, yield stress of the solid, coefficient of wear and the lubrication regime. For this reason it was decided to have finer time-steps in the beginning of the contact, due to higher plastic deformations, and have bigger time steps following that. Hence over the first 100 load cycles, the geometry was updated after every loading cycle. Thereafter the geometry was modified after every 100 loading cycles to increase the time efficiency of the simulations. The numerical model follows a semi-deterministic approach so that some parameters in the model should be calibrated prior to any predictions. One important

calibration parameter is the initial coefficient of wear ($^{K_{steel}}/_{H}$) used in the wear model. The other important parameters in the model are the tribofilm growth model parameters of Equation 5. These parameters (x_{tribo}, h_{max}, C_3 and C_4) are obtained by fitting the mathematical expression of Equation 1 to experimental tribofilm thickness results.

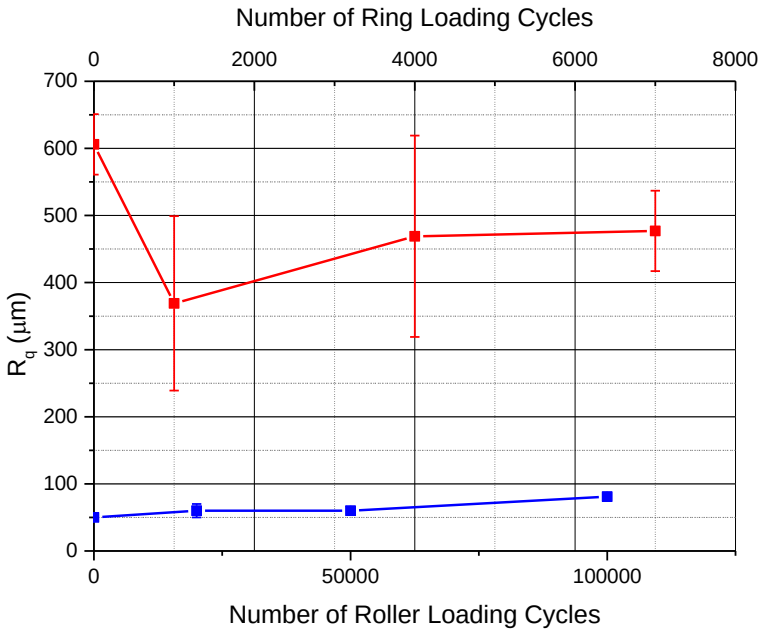

Figure 5 Experimental results of roughness measurements for initial Rq of 600 nm for the ring

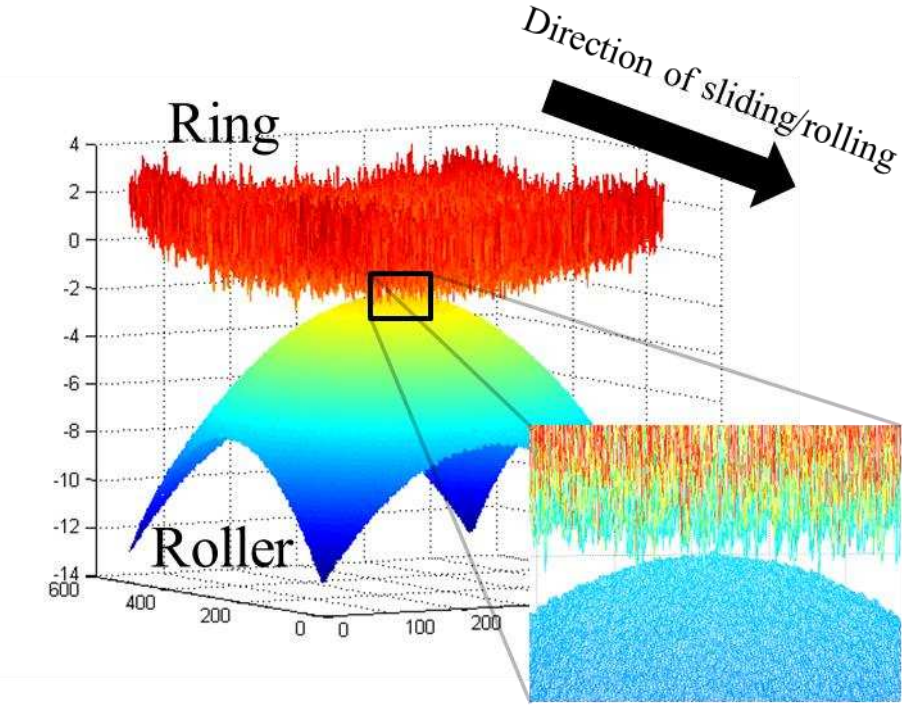

Figure 6 Configuration of MPR surfaces in the numerical model

All these calibration parameters were obtained from the previous work of the authors [28] and are reported in Table 1. Simulation results of the evolution of the surface roughness for the case of $R_q$rings=600 nm are plotted in Figure 7. Results show good qualitative and quantitative agreements with the experimental results shown in Figure 5. An example of the predicted tribofilm growth that shows patchiness of the layers formed on the rings are presented in Figure 8. Later in this paper, the same model (including model parameters) is employed to investigate the effect of tribofilm yield strength and its kinetics on the roughness evolution. It was shown in our previous paper that growth of the tribofilm on the contacting asperities can affect the roughness evolution and the detailed discussion around this point was presented. Therefore in this paper, a more thorough investigation on the effect of tribofilm kinetics and the hardness has been carried out. It should be noted that only one roughness parameter (R_q)was investigated in this work. However it is well-known that characterising surface roughness needs a thorough investigation of all the parameters such as skewness, kurtosis, slope of surface roughness etc. There are current research undergoing in the tribology community highlighting the importance of such parameters on the real area of contact and stickiness [41, 42]. These parameters should be considered in characterising the surface roughness. However in this paper only $R_q$has been considered and investigating the effect of other parameters will be the subject of future works.

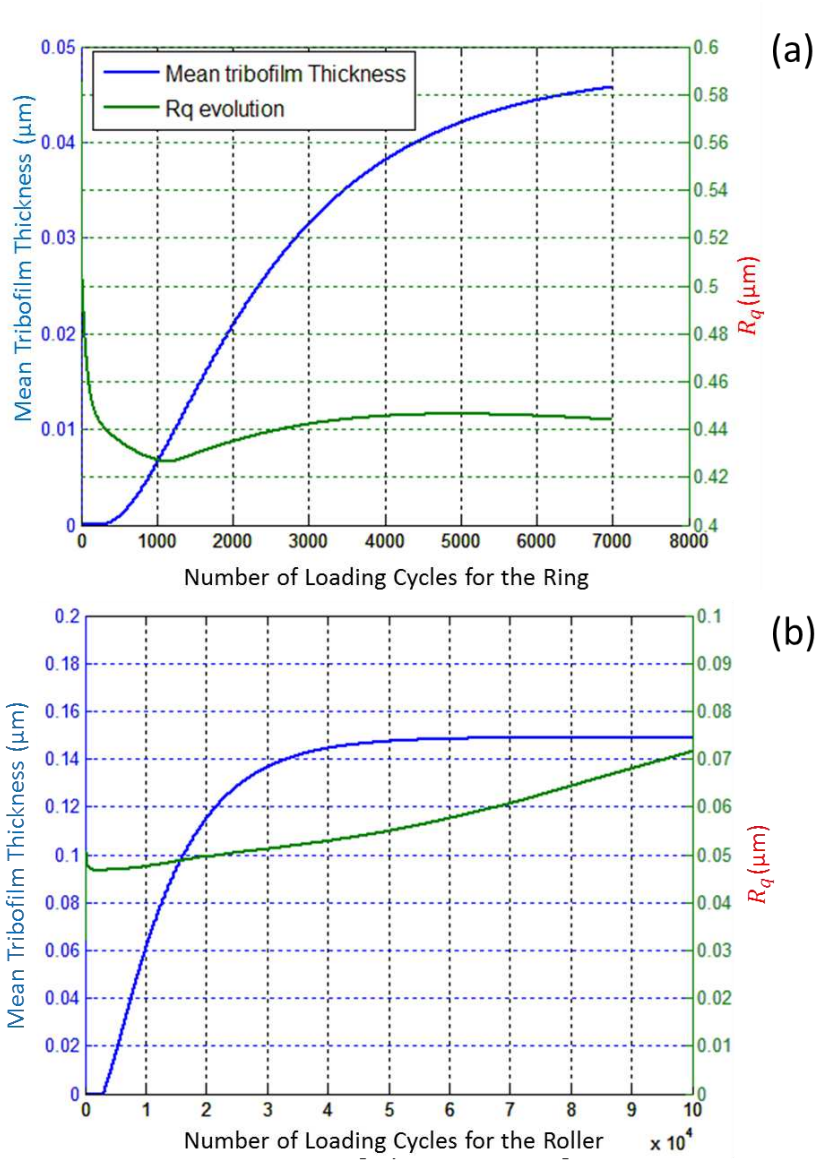

Figure 7 Simulations for validation of roughness evolution and the tribofilm growth for (a) the ring and (b) the roller

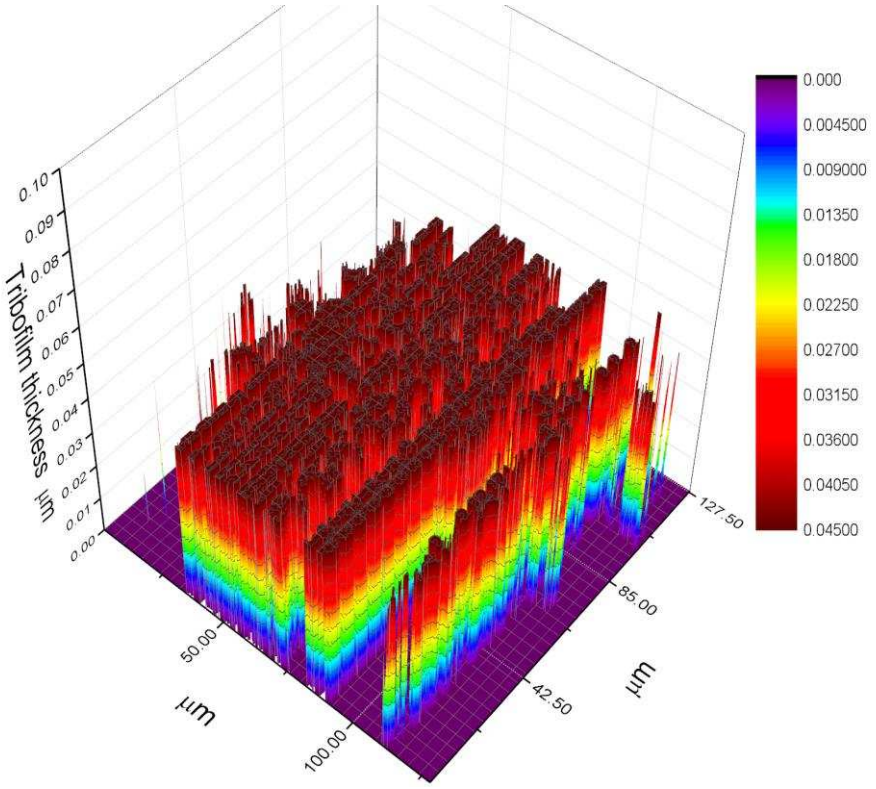

Figure 8 Example of the patchy tribofilm predicted by the numerical model and formed on the ring.

Table 1 Parameters used in the numerical simulation

Parameter	Value	Description
K_{steel}/H	1.25×10^{-17}	Dimensional wear coefficient for steel (m^3/Nm)
K_{min}/H	1.25×10^{-18}	Dimensional wear coefficient for maximum film thickness (m^3/Nm)
h_{max}	176	Maximum local tribofilm thickness in the formation process (nm)
C_3	0.112	Tribofilm removal constant
C_4	6.80×10^{-4}	Tribofilm removal exponential factor

5 Effect of the tribofilm kinetics and hardness on roughness evolution

5.1 Effect of tribofilm formation kinetics

Contact spots normally experience different shear forces due to inhomogeneity of force and other physical and chemical conditions and therefore might experience different reaction rates. In this model, there is no means of accommodating different shear stresses at different contacting spots. In order to study the effect of external forces on the kinetics of tribochemical reactions, simulations were conducted for different values of x_{tribo}. As discussed earlier in

Section 2.2, this term in principle, is a numerical representation of the effect of entropy change on the induction of the tribochemical reactions. Therefore changing the value of x_{tribo} in the kinetics model of Equation 5 enables the study of the effect of entropy on the kinetics of tribochemical reaction and therefore on the roughness evolution. It is important to highlight that any external force that can reduce the barrier of chemical reactions will contribute towards kinetics of tribochemical reactions [26]. These values are not adapted from any experiments and are only altered numerically in the model. The values are chosen to be close to the previously adapted values from experiments but altered in a range of one order of magnitude to investigate its effect. This term appears on the exponent of the Equation 5 and is therefore responsible for the rate of the tribochemical reaction kinetics and the corresponding film formation. This means that keeping all other parameters the same and only changing the rate of formation of the tribofilm (x_{tribo}) to investigate the effects on the topography evolution. Studying the effect of shear stress on the term x_{tribo} can be subject of future studies in order to present a more universal model. This can be conducted by ab-initio studies of tribochemical reactions and calculations of entropy change.

The values of x_{tribo} used in the numerical simulations are reported in Table 2. The evolution of surface roughness was then predicted by means of the model and the results are plotted in Figure 9. Simulation results suggest that the kinetics of ZDDP tribofilm formation significantly affect the roughness evolution of surfaces at different stages. Different stages of roughness evolution have been shown in Figure 10 for the case of $x_{tribo} = 4 \times 10^{-16}$. The changes in surface roughness have been divided into three main parts. Stage (i) which is the plastically-dominant part and the changes in the surface roughness occur quickly due to the high plastic deformations at the start of severe contact. This is followed by Stage (ii) in which tribofilm is formed on the surface and its mechanical properties significantly influence the conformity of the contact. As shown in Figure 9, the surfaces become rougher in the presence of tribofilm, which acts as a solid-like material. Finally, in Stage (iii), once the tribofilm growth rate decreases, the roughness evolution mainly occurs due to the mild wear at asperity-level. Results support the hypothesis that growth and kinetics of the antiwear tribofilm can affect the roughness evolution at Stage (ii) and this can -on its own- considerably influence the surface topography changes. It can be seen that at stage (iii), the R_q value is not decreasing and it can be attributed to the existing effect of tribofilm growth. It takes time for the effect of mild wear to be dominant and decrease the value of R_q. However it is observed that the rate of increase in the R_q value drops

and eventually this rate gets to zero (where the slope of R_q is zero). From this point onwards, mild wear will result in decreasing the value of R_q.

Once the tribofilm forms on the contact asperities, the topography of the surfaces is changed and the contact conditions between surfaces may change as a result. This change in the contact conditions can lead to a different topographical evolution at the interface in comparison to the case when no such tribofilm is formed. This effect can be seen in the numerical results of Figure 9. The tribofilm formed on the surfaces will change the local mechanical properties of the surfaces as well as their micro-geometry. An increase in the roughness of the rougher surface can occur because of the growth of the tribofilm, which is a solid-like material [43-48]. Fast growth of the tribofilm on the highest asperities in the running-in stage changes the geometry of those asperities in the contact (ring). The new asperity consists of a substrate (steel) and the glassy polyphosphate tribofilm on top [49]. It can come into contact with the counterbody (roller) and increase the average peak-to-valley height difference. The counter body also consists of a tribofilm on top but, in the running-in stage, there is a chance that some asperities are not covered by the tribofilm yet [50]. This will lead to the contact of the high asperities consisting of tribofilm into the asperities of the counterbody that are not yet covered by the tribofilm. After some time, the surface becomes gradually smoother because of the mild wear occurring at the contacting asperities. It can be seen that in the case of $x_{tribo} = 1 \times 10^{-15}$, the formation of the tribofilm is quicker than other cases and the geometry changes rapidly and some plastic deformation is happening. Therefore a slight reduction in the roughness is observed even at the second stage.

Table 2 Values of the x_{tribo} used in the numerical simulations

Parameter	Value	Description
x_{tribo}	1×10^{-16}; 2×10^{-16}; 4×10^{-16}; 7×10^{-16}; 1×10^{-15}	Tribofilm formation rate constant

The results of average wear depth for all cases are listed in Table 3. Figure 11 shows how the tribofilm is evolving on the ring and the corresponding surface topography at the end of the 7000 cycles. For comparison purposes, only a 37.5×37.5 μm^2 area in the middle of the wear track is shown. Results suggest that higher rates of tribofilm growth make the interface rougher

and prevent more smoothening of the rougher surface at some time period during running-in. Smoothening of surfaces is known to be a key factor in conformity of surfaces and running-in [6, 8]. In this paper, we have only reported the average wear depth of the surfaces and no attention is given to the micropitting phenomena. It should be noted that rougher surfaces may enhance micropitting and thus fatigue of the roller element bearing [40, 51]. In the future work, the effect of tribofilm and roughness on the sub-surface contact pressure history and initiation of surface micro-pits will be investigated.

Table 3 Values of the substrate average wear depth for different tribofilm kinetics

Parameter	x_{tribo}	Average wear depth (nm)
Values	1×10^{-16}	155
	2×10^{-16}	150
	4×10^{-16}	135
	7×10^{-16}	127
	1×10^{-15}	125

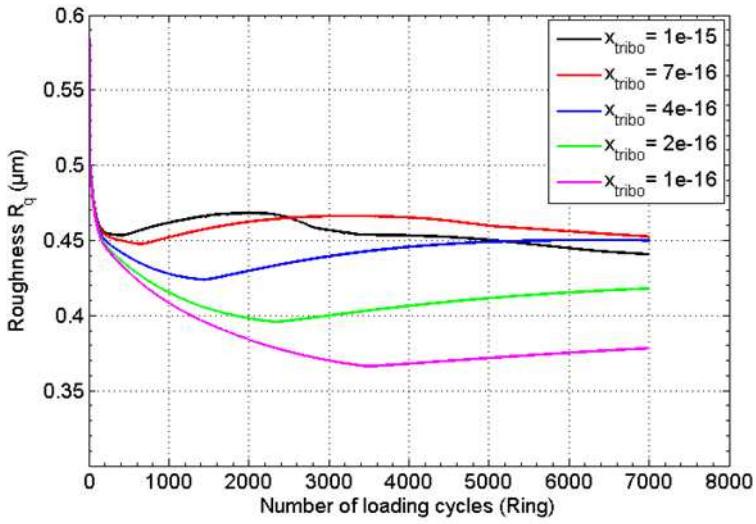

Figure 9 Effect of the tribofilm kinetics rate on the surface roughness evolution

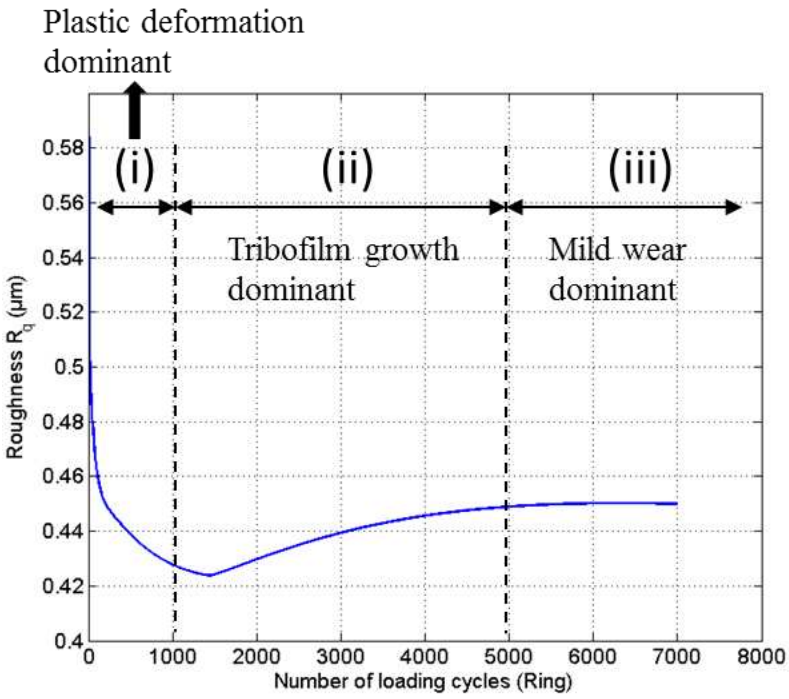

Figure 10 Different stages of roughness evolution in boundary lubrication in presence of ZDDP

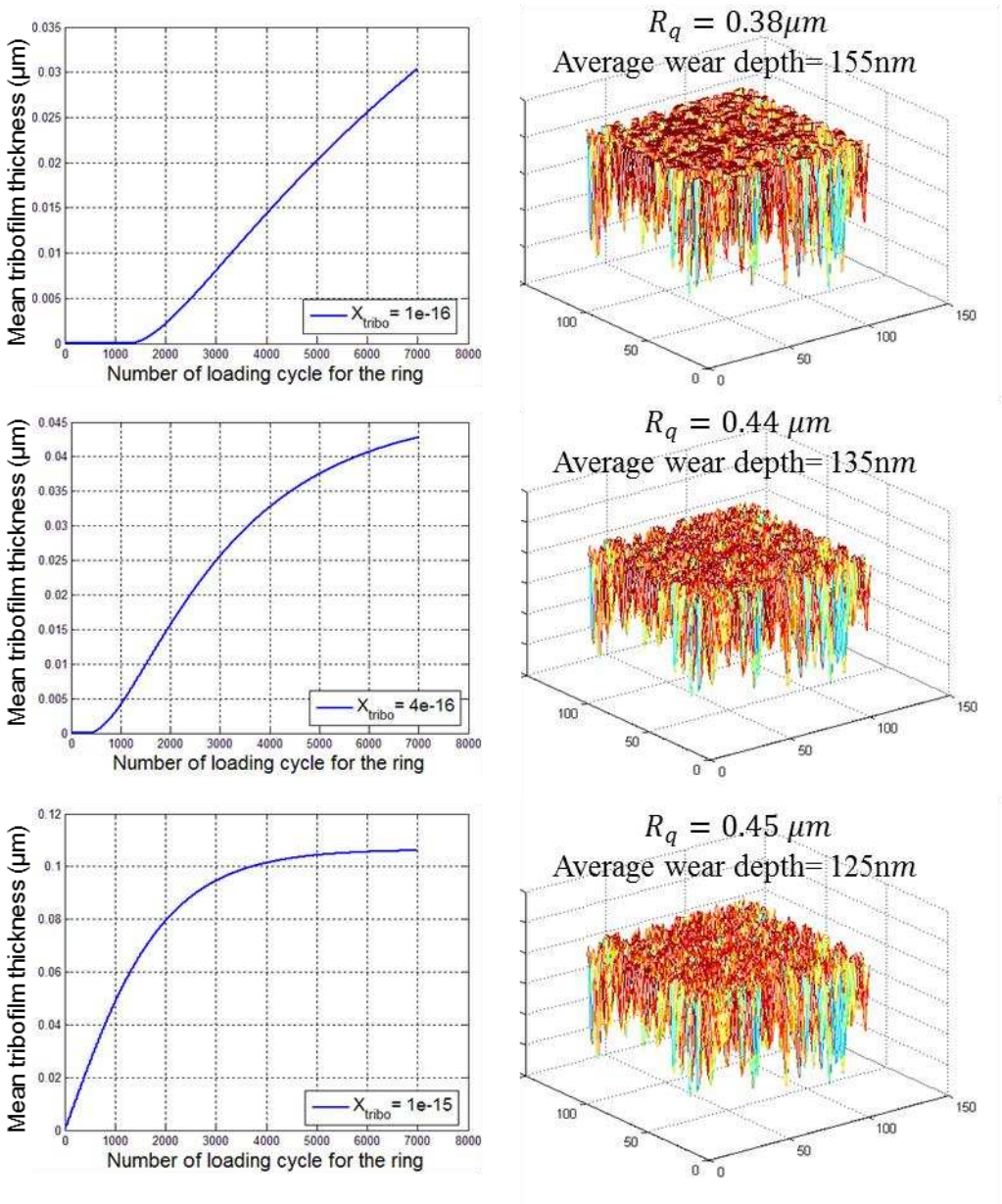

Figure 11 Simulation results of tribofilm evolution for different kinetics and the final surface topography in the middle of wear track (only an area in the middle of wear track is chosen for comparison purposes)

5.2 Effect of tribofilm hardness

Mechanical properties of the tribofilm seem to be important when it comes to the tribofilm separating the two substrates and protecting them since the mechanical properties play an important role in the contact and rubbing of surfaces. Hardness of the surfaces are known to be essential in determining the wear of rubbing surfaces both in two-body and three-body wear mechanisms. Therefore, investigating the effect of tribofilm hardness on the evolution of roughness is reasonable. The growth of the tribofilm is assumed to occur only at contacting asperities. Therefore the local contact properties calculated from the contact model are

responsible for the formation of the tribofilm at the asperity scale. It is observed experimentally that the formation of the tribofilm on asperities can lead to change in the mechanical properties of interfaces and also results in an increase in load-carrying capacities of the contacting bodies [43]. The tribofilm has been reported as a solid-like material with different hardness from the substrate [52-54]. The difference in the hardness of ZDDP tribofilm at different areas in the bulk was related to the different chain lengths of polyphosphate, with shorter polyphosphates being present deeper in the tribofilm and longer chains existing close to the surface of the film [49, 50, 55-57]. In the current model, the values of the tribofilm hardness at the surface and near the substrate can be approximated from experimental results available in the literature[45]. This variation was assumed to be between 2 and 6 GPa, in the previous studies [22, 28] changing linearly from the surface to the substrate. It is very challenging to measure the mechanical properties of such thin films especially when they have varying properties across their thickness. However in a recent work, authors have shown the stability and durability of tribofilms after replacing the oil [49]. This is a gross assumption but, given the lack of experimental data on the specific form of this variation, it seems reasonable. In addition, the elastic properties of the tribofilm also vary from the surface to the bulk and this variation is related to hardness variations [44].

In this work, the minimum value of the tribofilm hardness (at its maximum thickness) is changed numerically in the model and the effect on the roughness evolution is evaluated.

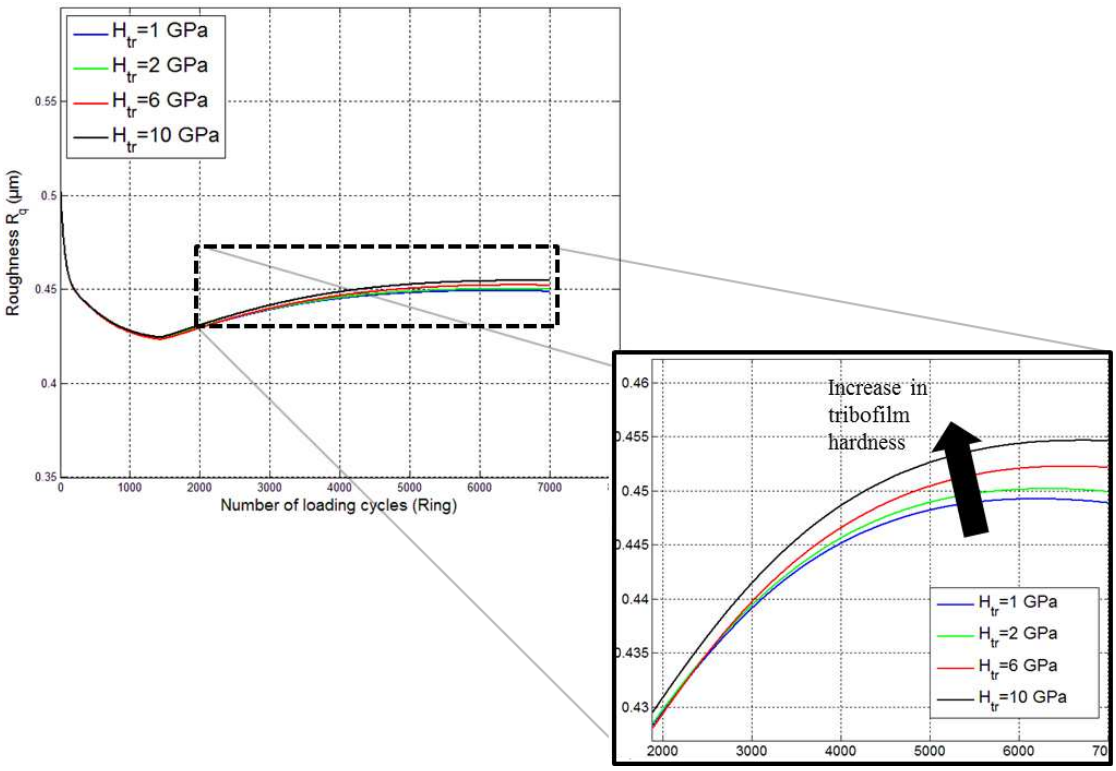

Figure 12 Effect of tribofilm hardness on the changes in surface roughness

Figure 12 shows the results of tribofilm evolution for different values of H_{tr}. Results suggest that the hardness of the tribofilm influences the surface roughness and this becomes dominant at the stage (ii) of roughness evolution when the tribofilm growth is dominant (see Figure 10 and Figure 12). This is in-line with the discussion presented in Section 5.1 that the growth of a solid-like material at the interface (a rougher interface) can increase the peak-to-valley distance. It can be noted that this effect is relatively insignificant and changing the hardness of the tribofilm for one order of magnitude will only result in 10nm difference in the R_q value of the underlying material. This is an interesting finding. This is because formation of the tribofilm will take time (in order of a few minutes) to reach to a relatively large thickness. When the tribofilm reaches the high thickness, the hardness will be the H_{tr} value. In this time instant, the surfaces already have run-in and the conformity of the surfaces is high and the changes in the topography will be minimum. On the other hand, in the running-in stage, where most of the topographical changes occur, the tribofilm is not grown to the thickness that its hardness will be able to influence the contact significantly. Therefore the effect of tribofilm hardness may become more dominant in stage (iii) where the mild wear is mainly responsible for the topography evolution. It should be noted that , in the previous paper of the authors [28], the effect of substrate hardness was investigated and was shown to significantly affect its

roughness evolution. This is not surprising, since harder materials are more resistant to mechanical wear based on most of traditional wear laws.

6 Conclusions

A tribochemical model that considers quasi-static contact of rough surfaces along with a growth kinetics model of tribofilm is used in this work. The development of the model was presented in other works of the authors. The kinetics model was initially developed for any lubricant additive that is involved in tribochemical reactions in boundary and mixed lubrication. However the wear model might be valid for some of P-containing antiwear additives where interfacial tribofilms physically act as barriers to direct asperity-asperity contacts and tribochemical wear becomes prominant. The model was previously validated against experimental results of an MPR in terms of surface roughness and tribofilm growth predictions. In this work, the effect of tribofilm kinetics and its hardness are investigated for the same MPR contact configurations and running conditions and the following conclusions are made:

- Kinetics of the growth of the tribofilm considerably affects the roughness evolution with higher growth rate resulting in more roughening of the surfaces at stage (ii).
- The tribofilm mechanical properties (hardness in this study) slightly affect the roughness evolution especially from stage (ii) where the tribofilm thickness is comparable to surface roughness. This effect found to be relatively insignificant (see Figure 12). However it can be seen that this effect will become gradually more important where mild wear mainly contributes to the surface topography in stage (iii).

Findings of this research might be of interest for interface designers to tune the kinetics and mechanical properties of tribolayer to engineer the evolution of surface roughness and severity of contact. Design of certain lubricant additives that results in the formation of tribofilms with desired mechanical properties may become a control parameter.

References

[1] Vakis, A. I., Yastrebov, V. A., Scheibert, J., Nicola, L., Dini, D., Minfray, C., Almqvist, A., Paggi, M., Lee, S., Limbert, G., Molinari, J. F., Anciaux, G., Aghababaei, R., Echeverri Restrepo, S., Papangelo, A., Cammarata, A., Nicolini, P., Putignano, C., Carbone, G., Stupkiewicz, S., Lengiewicz, J., Costagliola, G., Bosia, F., Guarino, R., Pugno, N. M., Müser, M. H., and Ciavarella, M., 2018, "Modeling and simulation in tribology across scales: An overview," Tribology International, 125, pp. 169-199.

[2] Meng, H., and Ludema, K., 1995, "Wear models and predictive equations: their form and content," Wear, 181, pp. 443-457.

[3] Meng, H.-C., 1994, "Wear modeling: evaluation and categorization of wear models," PhD, THE UNIVERSITY OF MICHIGAN.

[4] Dowson, D., 2006, "Tribological principles in metal-on-metal hip joint design," Proceedings of the Institution of Mechanical Engineers, Part H: Journal of Engineering in Medicine, 220(2), pp. 161-171.

[5] Stolarski, T., 2000, Tribology in machine design, Butterworth-Heinemann.

[6] Blau, P. J., 2006, "On the nature of running-in," Tribology International, 38(11), pp. 1007-1012.

[7] Blau, P. J., 1987, "A model for run-in and other transitions in sliding friction," Journal of tribology, 109(3), pp. 537-543.

[8] Blau, P. J., 1991, "Running-in: Art or engineering?," Journal of materials engineering, 13(1), pp. 47-53.

[9] Karpinska, A., 2010, "Running-in and the evolution of metallic surfaces subjected to sliding and rolling contact," Imperial College London.

[10] V Hegadekatte, Huber, N., and Kraft, O., 2005, "Finite element based simulation of dry sliding wear," modelling and simulation in materials science and engineering, 13(1), p. 57.

[11] Hegadekatte, V., Kurzenha, S., Huber, N., and Kraft, O., 2008, "A predictive modeling scheme for wear in tribometers," Tribology international, 41(11), pp. 1020-1031.

[12] Hegadekatte, V., Hilgertb, J., Kraft, O., and Huber, N., 2010, "Multi time scale simulations for wear prediction in micro-gears," Wear, 268(1), pp. 316-324.

[13] Öqvist, M., 2001, "Numerical simulations of mild wear using updated geometry with different step size approaches," wear, 249(1), pp. 6-11.

[14] Andersson, J., Almqvist, A., and Larsson, R., 2011, "Numerical simulation of a wear experiment," Wear, 271(11), pp. 2947-2952.

[15] Furustig, J., Almqvist, A., Bates, C., Ennemark, P., and Larsson, R., 2015, "A two scale mixed lubrication wearing-in model, applied to hydraulic motors," Tribology International, 90, pp. 248-256.

[16] Furustig, J., Dobryden, I., Almqvist, A., Almqvist, N., and Larsson, R., 2016, "The measurement of wear using AFM and wear interpretation using a contact mechanics coupled wear model," Wear, 350, pp. 74-81.

[17] Ezawa, Y., and Okamoto, N., 1995, "Development of contact stress analysis programs using the hybrid method of FEM and BEM," Computers & structures, 57(4), pp. 691-698.

[18] Ilincic, S., Vorlaufer, G., Fotiu, P. A., Vernes, A., and Franek, F., 2009, "Combined finite element-boundary element method modelling of elastic multi-asperity contacts," Proceedings of the Institution of Mechanical Engineers, Part J: Journal of Engineering Tribology, 223(5), pp. 767-776.

[19] Bosman, R., and Schipper, D., 2011, "Mild wear prediction of boundary-lubricated contacts," Tribology letters, 42(2), pp. 169-178.

[20] Bosman, R., and Schipper, D. J., 2011, "Running-in of systems protected by additive-rich oils," Tribology Letters, 41(1), pp. 263-282.

[21] Andersson, J., Larsson, R., Almqvist, A., Grahn, M., and Minami, I., 2012, "Semi-deterministic chemo-mechanical model of boundary lubrication," Faraday discussions, 156(1), pp. 343-360.

[22] Ghanbarzadeh, A., Parsaeian, P., Morina, A., Wilson, M. C., van Eijk, M. C., Nedelcu, I., Dowson, D., and Neville, A., 2016, "A Semi-deterministic Wear Model Considering the Effect of Zinc Dialkyl Dithiophosphate Tribofilm," Tribology Letters, 61(1), pp. 1-15.
[23] Akchurin, A., and Bosman, R., 2017, "A deterministic stress-activated model for tribo-film growth and wear simulation," Tribology letters, 65(2), p. 59.
[24] Zhang, J., and Spikes, H., 2016, "On the mechanism of ZDDP antiwear film formation," Tribology Letters, 63(2), pp. 1-15.
[25] Spikes, H., and Tysoe, W., 2015, "On the commonality between theoretical models for fluid and solid friction, wear and tribochemistry," Tribology Letters, 59(1), p. 21.
[26] Tysoe, W., 2017, "On stress-induced tribochemical reaction rates," Tribology Letters, 65(2), p. 48.
[27] Ghanbarzadeh, A., Wilson, M., Morina, A., Dowson, D., and Neville, A., 2016, "Development of a New Mechano-Chemical Model in Boundary Lubrication," Tribology International, 93, pp. 573-582.
[28] Ghanbarzadeh, A., Piras, E., Nedelcu, I., Brizmer, V., Wilson, M. C. T., Morina, A., Dowson, D., and Neville, A., 2016, "Zinc Dialkyl Dithiophosphate Antiwear Tribofilm and its Effect on the Topography Evolution of Surfaces: A Numerical and Experimental Study," Wear, 362-363, pp. 186-198.
[29] Bhushan, B., and Majumdar, A., 1992, "Elastic-plastic contact model for bifractal surfaces," Wear, 153(1), pp. 53-64.
[30] Blok, H., 1963, "The flash temperature concept," Wear, 6(6), pp. 483-494.
[31] Tian, X., and Kennedy, F. E., 1994, "Maximum and average flash temperatures in sliding contacts," Journal of Tribology, 116(1), pp. 167-174.
[32] Bulgarevich, S., Boiko, M., Kolesnikov, V., and Korets, K., 2010, "Population of transition states of triboactivated chemical processes," Journal of Friction and Wear, 31(4), pp. 288-293.
[33] Bulgarevich, S., Boiko, M., Tarasova, E., Feizova, V., and Lebedinskii, K., 2012, "Kinetics of mechanoactivation of tribochemical processes," Journal of Friction and Wear, 33(5), pp. 345-353.
[34] Bulgarevich, S., Boiko, M., Kolesnikov, V., and Feizova, V., 2011, "Thermodynamic and kinetic analyses of probable chemical reactions in the tribocontact zone and the effect of heavy pressure on evolution of adsorption processes," Journal of Friction and Wear, 32(4), pp. 301-309.
[35] Bosman, R., and Schipper, D. J., 2011, "Mild Wear Prediction of Boundary-Lubricated Contacts," Tribology Letters, 42(2), pp. 169-178.
[36] Chen, W. W., Liu, S., and Wang, Q. J., 2008, "Fast Fourier transform based numerical methods for elasto-plastic contacts of nominally flat surfaces," Journal of Applied Mechanics, Transactions ASME, 75(1), pp. 110221-1102211.
[37] Liu, S., Hua, D., Chen, W. W., and Wang, Q. J., 2007, "Tribological modeling: application of fast Fourier transform," Tribology international, 40(8), pp. 1284-1293.
[38] Liu, S., Wang, Q., and Liu, G., 2000, "A versatile method of discrete convolution and FFT (DC-FFT) for contact analyses," Wear, 243(1–2), pp. 101-111.
[39] Topolovec-Miklozic, K., Forbus, T. R., and Spikes, H. A., 2007, "Film thickness and roughness of ZDDP antiwear films," Tribology Letters, 26(2), pp. 161-171.
[40] Morales-Espejel, G. E., Brizmer, V., and Piras, E., 2015, "Roughness evolution in mixed lubrication condition due to mild wear," Proceedings of the Institution of Mechanical Engineers, Part J: Journal of Engineering Tribology, 229(11), pp. 1330-1346.
[41] Pastewka, L., and Robbins, M. O., 2014, "Contact between rough surfaces and a criterion for macroscopic adhesion," Proceedings of the National Academy of Sciences, p. 201320846.
[42] Müser, M. H., Dapp, W. B., Bugnicourt, R., Sainsot, P., Lesaffre, N., Lubrecht, T. A., Persson, B. N., Harris, K., Bennett, A., and Schulze, K., 2017, "Meeting the contact-mechanics challenge," Tribology Letters, 65(4), p. 118.
[43] Aktary, M., McDermott, M. T., and McAlpine, G. A., 2002, "Morphology and nanomechanical properties of ZDDP antiwear films as a function of tribological contact time," Tribology letters, 12(3), pp. 155-162.
[44] Demmou, K., Bec, S., Loubet, J.-L., and Martin, J.-M., 2006, "Temperature effects on mechanical properties of zinc dithiophosphate tribofilms," Tribology international, 39(12), pp. 1558-1563.

[45] S. Bec, A. Tonck, J. M. Georges, R. C. Coy, Bell, J. C., and Roper, G. W., 1999, "Relationship between mechanical properties and structures of zinc dithiophosphate anti-wear films," Proceedings of the Royal Society A: Mathematical, Physical and Engineering Science, 445(1992), pp. 4181-4203.
[46] Pereira, G., Lachenwitzer, A., Nicholls, M. A., Kasrai, M., Norton, P. R., and Stasio, G. D., 2005, "Chemical characterization and nanomechanical properties of antiwear films fabricated from ZDDP on a near hypereutectic Al–Si alloy," Tribology Letters, 18(4), pp. 411-427.
[47] J.F. Graham, McCague, C., and Norton, P. R., 1999, "Topography and nanomechanical properties of tribochemical films derived from zinc dialkyl and diaryl dithiophosphates," Tribology Letters, 6(3-4), pp. 149-157.
[48] Ye, J., Kano, M., and Yasuda, Y., 2002, "Evaluation of local mechanical properties in depth in MoDTC/ZDDP and ZDDP tribochemical reacted films using nanoindentation," Tribology Letters, 13(1), pp. 41-47.
[49] Parsaeian, P., Ghanbarzadeh, A., Van Eijk, M. C., Nedelcu, I., Neville, A., and Morina, A., 2017, "A new insight into the interfacial mechanisms of the tribofilm formed by zinc dialkyl dithiophosphate," Applied Surface Science, 403, pp. 472-486.
[50] Spikes, H., 2004, "The history and mechanisms of ZDDP," Tribology Letters, 17(3), pp. 469-489.
[51] Morales-Espejel, G. E., and Brizmer, V., 2011, "Micropitting modelling in rolling–sliding contacts: Application to rolling bearings," tribology transactions, 54(4), pp. 625-643.
[52] Nehme, G., Mourhatch, R., and Pranesh B. Aswath, 2010, "Effect of contact load and lubricant volume on the properties of tribofilms formed under boundary lubrication in a fully formulated oil under extreme load conditions," Wear, 268(9), pp. 1129-1147.
[53] Mourhatch, R., and Aswath, P., 2011, "Tribological behavior and nature of tribofilms generated from fluorinated ZDDP in comparison to ZDDP under extreme pressure conditions—Part II: Morphology and nanoscale properties of tribofilms," tribology international, 44(3), pp. 201-210.
[54] Nicholls, M. A., Nortona, P. R., Bancroft, G. M., M. Kasrai, T. Dob, Frazerc, B. H., and Stasio, G. D., 2004, "Nanometer scale chemomechanical characterization of antiwear films," Tribology Letters, 17(2), pp. 205-216.
[55] Crobu, M., Rossi, A., Mangolini, F., and Spencer, N. D., 2010, "Tribochemistry of bulk zinc metaphosphate glasses," Tribology letters, 39(2), pp. 121-134.
[56] Yin, Z., Kasrai, M., Fuller, M., Bancroft, G. M., Fyfe, K., and Tan, K. H., 1997, "Application of soft X-ray absorption spectroscopy in chemical characterization of antiwear films generated by ZDDP Part I: the effects of physical parameters," Wear, 202(2), pp. 172-191.
[57] Martin, J. M., Grossiord, C., Le Mogne, T., Bec, S., and Tonck, A., 2001, "The two-layer structure of Zndtp tribofilms: Part I: AES, XPS and XANES analyses," Tribology international, 34(8), pp. 523-530.

List of Figures